

Nano Science and Nano Technology

An Indian Journal

Full Paper

NSNTAIJ, 8(7), 2014 [265-273]

Nano-sized metal 1,3-di(4-pyridyl)propane coordination polymer prepared via the surface layer-by-layer chemical deposition method

Aref A.M.Aly^{1*}, Maged S.Al-Fakeh², Mahmoud A.Ghandour¹

¹Faculty of Science, Department of Chemistry, Assiut University, 71516 Assiut, (EGYPT)

²Faculty of Science, Taiz University, Taiz, (YEMEN)

E-mail : aref_20002001@yahoo.com; maged7969@yahoo.com

ABSTRACT

Five new metal coordination polymers of the general formula $\{[M(DPP)(H_2O)_mX].xH_2O\}_n$, (M = Mn(II), Co(II), Cu(II), Cd(II) and Pb(II), m = 0 or 2, X = Cl⁻ or NO₃⁻, x = 2 or 5, DPP = 1,3-di(4-pyridyl) propane have been prepared by the thin film surface layer-by-layer chemical deposition reaction. The coordination polymers have been characterized based on elemental analysis, FT-IR and electronic spectral studies, thermal analysis, X-ray powder diffraction and biological activity. Thermogravimetry (TG), derivative thermogravimetry (DTG) and differential thermal analysis (DTA) have been used to study the thermal decomposition steps. The kinetic parameters have been calculated making use of the Coats-Redfern and Horowitz-Metzger equations. The scanning electron microscope (SEM) measurements and the calculations on the powder XRD data indicate the nano-sized nature of the prepared supramolecular coordination polymers. The oxides CuO and PbO nano-particles were characterized by X-ray diffraction (XRD), (SEM) and (TEM) (average particle size 19-36 nm).

© 2014 Trade Science Inc. - INDIA

KEYWORDS

Nano-sized coordination polymers;
Layer-by-layer chemical deposition;
Characterization.

INTRODUCTION

Supramolecular coordination polymers have attracted much attention in recent years due to their complicated topological structures and intriguing magnetic, catalytic, luminescent and optical properties^[1-4]. They represent an important interface between synthetic chemistry and material science. Nanometer-sized particles of metal coordination polymers are of interest to explore, since their unique properties are controlled by the large number of surface molecules, leading to an entirely different environment than those in a bulk crystal^[5]. Therefore, they are of potential use as materials

for nanotechnological applications. However, their use as precursors for the preparation of inorganic nanomaterials has not been thoroughly investigated^[6]. Currently, more research efforts have been devoted to the beneficial applications of the layer-by-layer deposition technique. This methodology has emerged and been found a more economic alternative for the direct preparation of thin films^[7-9]. Synthesis of a variety of important compounds was successfully achieved via the layer-by-layer thin film deposition approach^[10]. In addition, it is known that the flexible nitrogen donor ligand 1,3-di(4-pyridyl) propane (DPP) is used in the construction of coordination polymers that can show a wide

Full Paper

range of interesting topologies as chains, ladders, grids and adamantoid networks^[11]. The ligand is a bipyridyl analog with a $-\text{CH}_2\text{CH}_2\text{CH}_2-$ spacer which imports to it a considerable flexibility. Furthermore, the longer nitrogen to nitrogen span enhances larger cavities formation in the resulting networks and the variable conformations of DPP may lead to different extended structures^[12]. Reaction of $\text{Co}(\text{NO}_3)_2$ or $\text{Cd}(\text{NO}_3)_2$ with DPP in a mixture of benzene and methanol generates one dimensional coordination polymers of the formulas $\{[\text{Co}(\text{DPP})_2(\text{NO}_3)_2] \cdot 2\text{C}_6\text{H}_6\}_n$ and $\{[\text{Cd}(\text{DPP})_2(\text{NO}_3)_2] \cdot 2\text{C}_6\text{H}_6\}_n$ ^[12]. A three dimensional coordination polymer comprising Cd(II), NO_2^- and DPP was also synthesized with the formula $[\text{Cd}(\mu\text{-DPP})_3(\text{NO}_3)_4]_n$ ^[13]. Plater et al. reported a number of coordination polymers of Co(II), Ni(II) and Cd(II) with different topologies. These polymers which were synthesised in aqueous solutions have the formulas $\{[\text{Cd}_2(\text{NO}_3)_3(\text{DPP})_4(\text{H}_2\text{O})] \cdot \text{NO}_3\}_n$ and $\{[\text{M}(\text{DPP})_2(\text{H}_2\text{O})_2](\text{ClO}_4)_2 \cdot \text{DPP} \cdot \text{H}_2\text{O}\}_n$ (M= Co(II), Ni(II))^[14]. The ligand is also involved in a number of mixed ligand coordination polymers^[15-17]. In view of the above importance of this ligand and its complexes, we report in this work on the synthesis and characterization of manganese(II), cobalt(II), copper(II), cadmium(II) and lead(II) coordination polymers with DPP. Preparation and characterization of nano metal-oxides are also described.

EXPERIMENTAL

Materials and methods

The chemicals used were of analytical grade. 1,3-Di(4-pyridyl)propane (E. Aldrich) was purchased and used without purification.

Layer-by-layer thin film formation of 1,3-di(4-pyridyl)propane metal coordination polymers

The formation of the 1,3-di(4-pyridyl)propane metal coordination polymers was carried out by a chemical dipping method according to the following procedure. In this method, a clean glass micro-slide of the size 76.2 mm by 25.4 mm by 1 mm was used as the solid substrate. $\{[\text{Cu}(\text{DPP})\text{Cl}_2(\text{H}_2\text{O})_2] \cdot 4\text{H}_2\text{O}\}_n$ synthesis is typical. A methanolic solution (15 mL) of DPP ligand (0.2 g, 1 mmol) was prepared and the copper(II) chloride

was dissolved in 15 mL methanol (0.171 g, 1 mmol). The clean substrate was vertically immersed into the copper(II) chloride solution for 40 s period to adhere the a layer of $\text{CuCl}_2 \cdot 2\text{H}_2\text{O}$ on the substrate surface. The substrate was then immersed in the 1,3-di(4-pyridyl)propane solution for another 40 s, where the pre-adsorbed metal ion on the glass substrate reacts with the DPP ligand. Repeating this dipping cycle for a few times produced a colored and uniform thin film of the copper coordination polymer. The reaction substrate was carefully rinsed with distilled water and EtOH and left to dry in air.

Calcination of the coordination polymers

Two of the prepared polymers, namely 3 and 5 are subjected to calcination at 550 °C to afford CuO and PbO oxides, respectively.

Physical measurements

The stoichiometric analyses(C,H,N) were performed using Analytischer Funktionstest Vario El Fab-Nr.11982027 elemental analyzer. The conductance was measured using a conductivity Meter model 4310 JENWAY. The i.r spectra were recorded on a Shimadzu IR-470 spectrophotometer and the electronic spectra were obtained using a Shimadzu UV-2101 PC spectrophotometer. Thermal studies were carried out in dynamic air on a Shimadzu DTG 60-H thermal analyzer at a heating rate 10 °C min⁻¹. The X-ray diffractometer was a Philips 1700 version with H. T. P.W 1730 / 104 KVA and the anode was Cu K α ($\lambda = 1.54180 \text{ \AA}$). The scanning electron microscope was a JEOL JFC-1100E ION SPUTTERING DEVICE, JEOL JSM-5400LV. SEM specimens were coated with gold to increase the conductivity. Transmission electron microscope was of the type JEOL JEM-100CX II ELECTRON MICROSCOPE.

Biological activity

The antimicrobial activity of the complexes was tested against 5 bacterial and 5 fungal strains. These strains are common contaminants of the environment in Egypt and some of which are involved in human and animal diseases (*Candida albicans*, *Geotrichum candidum*, *Scopulariopsis brevicaulis*, *Aspergillus flavus*, *Staphylococcus aureus*), plant diseases (*Fusarium oxysporum*) or frequently reported from

contaminated soil, water and food substances (*Escherichia coli*, *Bacillus cereus*, *Pseudomonas aeruginosa* and *Serratia marcescens*). To prepare inocula for bioassay, bacterial strains were individually cultured for 48h in 100 ml conical flasks containing 30 ml nutrient broth medium. Fungi were grown for 7 days in 100 ml conicals containing 30 ml Sabouraud's dextrose broth. Bioassay was done in 10 cm sterile plastic Petri plates in which microbial suspension (1ml/plate) and 15 ml appropriate agar medium (15 ml/plate) were poured. Nutrient agar and Sabouraud's dextrose agar were respectively used for bacteria and fungi. After solidification of the media, 5 mm diameter cavities were cut in the solidified agar (4 cavities/plate) using sterile cork borer. The chemical compounds dissolved in dimethyl sulfoxide (DMSO) at 2% w/v (=20 mg/ml) were pipetted in the cavities (20 ul /cavity). Cultures were then incubated at 28°C for 48 h in case of bacteria and up to 7 days in case of fungi. The results were read as the diameter (in mm) of inhibition zone around cavities.

RESULTS AND DISCUSSION

The coordination polymers were prepared by the reaction of 1,3-di(4-pyridyl)propane and the metal salts. The prepared compounds were found to react in the molar ratio 1: 1 metal : DPP. The coordination polymers are air stable, insoluble in common organic solvents but partially soluble in DMSO. The conductivity was measured in DMSO using 10^{-3} M solutions of the complexes. Although the conductivities of these complexes are lower than reported for 1:1 electrolytes^[18], but their values refer to an extensive dissociation of the complexes in DMSO. The compositions of the coordination polymers are supported by the elemental analysis

and are recorded together with color and molar conductance values in TABLE 1. The structure of the ligand DPP is presented in Figure 1.

IR spectra

The most relevant infrared spectral bands of the coordination polymers are given in TABLE 2. The IR spectra of the prepared compounds show a band in the range 1606-1618 cm^{-1} characteristic of the $\nu\text{C}=\text{N}$ stretching vibrations of the DPP coordinated to the metal center^[19]. A band was found at 1385 cm^{-1} corresponding to the $\nu(\text{NO}_3)$ of compound 5^[20]. The bands at 3420-3440 cm^{-1} in the spectra of compounds 3, 4 and 5 are assigned to νOH of crystalline water molecules^[21], whereas the νOH stretching vibrations of coordinated water molecules are located in the range 3020-3122 cm^{-1} for these complexes^[22]. Metal-oxygen and metal-nitrogen bonding are manifested by the existence of bands in the 505-529 cm^{-1} and 416-434 cm^{-1} regions, respectively^[21]. Figure 2 illustrates the infrared spectrum of compound 3.

Electronic spectra and magnetic moments

The UV-Vis spectra of the coordination polymers

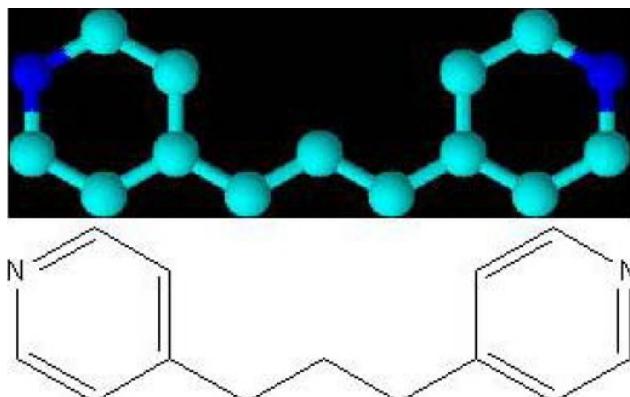


Figure 1 : Structure of DPP.

TABLE 1 : Physical properties and elemental analysis of the compounds

Compound	M.F(M.Wt)	Color	Found (Calcd. %)			m.p.°C (Decom.)	Λ_m $\text{Scm}^2 \text{mol}^{-1}$
			C	H	N		
[Mn(DPP)Cl ₂] _n 1	C ₁₃ H ₁₄ Cl ₂ MnN ₂ (324.13)	Light Brown	49.06 48.16	5.59 4.36	9.37 8.64	228	60.6
[Co(DPP)Cl ₂] _n 2	C ₁₃ H ₁₄ Cl ₂ CoN ₂ (328.12)	Dark Blue	48.09 47.58	4.96 4.30	9.04 8.53	212	57.8
{[Cu(DPP)Cl ₂ (H ₂ O) ₂].4H ₂ O} _n 3	C ₁₃ H ₂₆ Cl ₂ CuN ₂ O ₆ (440.86)	Greenish-blue	34.65 35.41	5.15 5.95	5.89 6.35	206	44.2
{[Cd(DPP)Cl ₂ (H ₂ O) ₂].H ₂ O} _n 4	C ₁₃ H ₂₀ Cl ₂ CdN ₂ O ₃ (435.66)	White	36.02 35.83	4.92 4.63	7.11 6.43	198	36.8
{[Pb(DPP)(NO ₃) ₂].2H ₂ O} _n 5	C ₁₃ H ₁₈ PbN ₄ O ₈ (565.55)	White	28.01 27.60	3.81 3.21	8.11 9.90	216	48.5

Full Paper

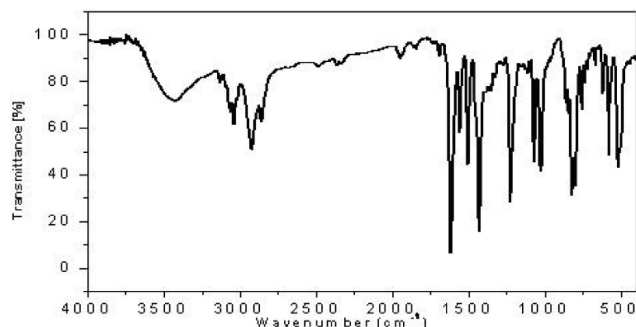


Figure 2 : FT-IR of compound 3

have been recorded in DMSO. The results are shown in TABLE 3. For all the compounds a band appears in the range 33,557-34,722 cm^{-1} which can be correlated with a $n \rightarrow \pi^*$ transition. However, the band occurring in the range 36,496-39,370 cm^{-1} is assigned to a $\pi \rightarrow \pi^*$ transition. The compounds, except 4 and 5 show broad bands with very low intensity in the range 25,000-12,000 cm^{-1} , which are assigned to the d-d transitions. For Mn(II), the magnetic moment value of 5.72 B.M is in agreement with the value reported for those of Mn(II) tetrahedral compounds^[23]. The magnetic moment value of 4.12 B.M for the Co(II) complex indicates a tetracoordination around Co(II)^[24]. In addition, the magnetic moment value of 1.85 B.M. confirms the paramagnetic nature of the Cu(II) complex and the octahedral geometry around Cu(II) ion^[25,26]. From the above

TABLE 2 : Infrared spectral data of the compounds

Compounds	ν (H ₂ O)	ν (NO ₃)	ν (C=N)	ν (M-N)	ν (M-O)
1	-	-	1610	420	-
2	-	-	1616	416	-
3	3280,3020	-	1618	432	520
4	3420,3122	-	1614	434	505
5	3440	1385	1606	426	529

TABLE 3 : Electronic spectral data and magnetic moments of the compounds

Compounds	ν_{max} (cm^{-1})	Assignment	μ_{eff} B.M
1	36,496	$\pi \rightarrow \pi^*$ transition	5.72
2	21,978	d-d transition	4.12
	36,630	$\pi \rightarrow \pi^*$ transition	
3	22,831	d-d transition	1.85
	33,557	$n \rightarrow \pi^*$ transition	
	38,022	$\pi \rightarrow \pi^*$ transition	
4	37,735	$\pi \rightarrow \pi^*$ transition	-
5	34,722	$n \rightarrow \pi^*$ transition	-
	39,370	$\pi \rightarrow \pi^*$ transition	

data the structure of the coordination polymers can be postulated as in Figure 3 and 4:

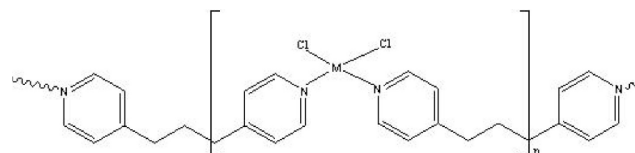
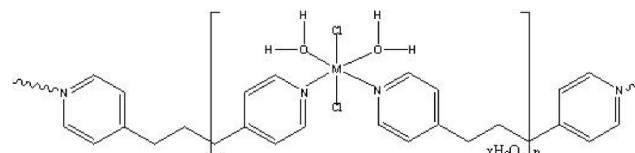
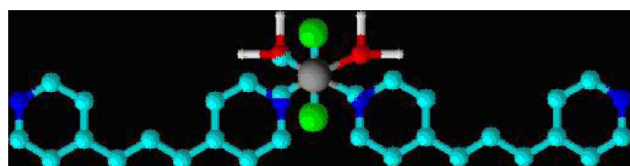
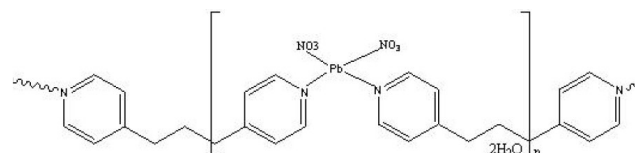
Figure 3(a) : Structure of $[M(\text{DPP})\text{Cl}_2]_n$, (M= Mn(II) and Co(II))Figure 3(b) : Structure of $\{[M(\text{DPP})(\text{H}_2\text{O})_2\text{Cl}_2] \cdot x\text{H}_2\text{O}\}_n$, (M= Cu(II) and Cd(II), x = 1 or 4)

Figure 3(c) : View of the complete coordination around the copper ions in the coordination polymers

Figure 4 : Structure of $\{[\text{Pb}(\text{DPP})(\text{NO}_3)_2] \cdot 2\text{H}_2\text{O}\}_n$

Thermal studies

The thermal decomposition of compounds 3 and 4 has been investigated in dynamic air from ambient temperature to 750 °C and the thermal data are cited in TABLE 4. As a representative example, the thermogram of the cadmium coordination polymer 4 is depicted in Figure 5. It shows four decomposition steps

TABLE 4 : Thermal decomposition data of compounds 3 and 4 in dynamic air

Compound	Step	TG/DTG			Mass Loss (%)
		Ti	Tm	Tf	
$\{[\text{Cu}(\text{DPP})\text{Cl}_2(\text{H}_2\text{O})_2] \cdot 4\text{H}_2\text{O}\}_n$ 3	1 st	42	116	179	1.74
	2 nd	180	263	319	21.76
	3 rd	320	337	393	5.77
	4 th	394	559	750	52.51
$\{[\text{Cd}(\text{DPP})\text{Cl}_2(\text{H}_2\text{O})_2] \cdot \text{H}_2\text{O}\}_n$ 4	1 st	48	240	282	11.92
	2 nd	283	370	388	10.25
	3 rd	389	431	490	16.94
	4 th	491	620	750	33.39

Ti=Initial temperature, Tm=Maximum temperature, Tf=Final temperature

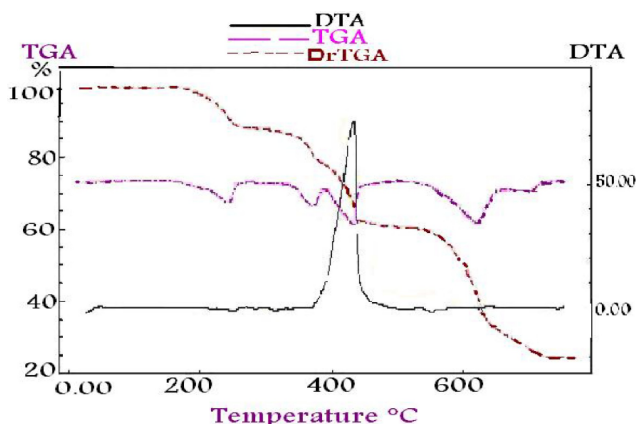
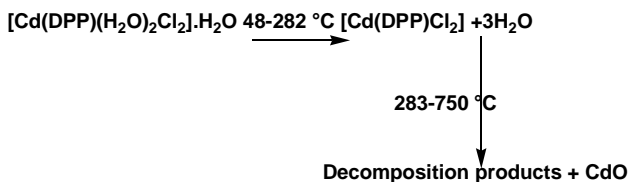


Figure 5 : TG, DTG and DTA thermograms of compound 4 in dynamic air

occurring in the temperature ranges 48-282, 283-388, 389-490 and 491-750 °C. In the first step the two coordinated water molecules and one crystalline water molecule are released (calc. 12.40 %, found 11.92 %). The corresponding DTG peak occurs at 242 °C and an endothermic peak appears at 244 °C in the DTA trace. The second, third and fourth steps are correlated with the decomposition products of the ligand (calc. 61.78 %, found 60.58 %) with corresponding three DTG peaks at 370, 431 and 622 °C and three exothermic peaks at 372, 433 and 625 °C in the DTA trace, respectively. The final product is assigned to the CdO (calc. 29.47 %, found 27.50%) (scheme 1).



Scheme 1

Kinetic analysis

Non-isothermal kinetic analysis of the coordination polymers was carried out applying two different procedures: the Coats-Redfern^[27] and the Horowitz-Metzger^[28] methods.

a) Coats-Redfern equation

$$\ln[1-(1-\alpha)^{1-n}/(1-n)T^2] = M/T + B \text{ for } n \neq 1 \quad (1)$$

$$\ln[-\ln(1-\alpha)/T^2] = M/T + B \text{ for } n = 1 \quad (2)$$

where α is the fraction of material decomposed, n is the order of the decomposition reaction and $M = -E/R$ and $B = ZR/\Phi E$; E , R , Z and Φ are the activation energy, gas constant, pre-exponential factor and heating rate,

respectively.

b) Horowitz-Metzger equation

$$\ln[1-(1-\alpha)^{1-n}/1-n] = \ln ZRT_s^2/\Phi E - E/RT_s + E\theta/RT_s^2 \text{ for } n \neq 1 \quad (3)$$

$$\ln[-\ln(1-\alpha)] = E\theta/RT_s^2 \text{ for } n = 1 \quad (4)$$

where $\theta = T - T_s$, T_s is the temperature at the DTG peak. The correlation coefficient r is computed using the least squares method for equations (1), (2), (3) and (4). Linear curves were drawn for different values of n ranging from 0 to 2. The value of n , which gave the best fit, was chosen as the order parameter for the decomposition stage of interest. The kinetic parameters were calculated from the plots of the left hand side of equations (1), (2), against $1/T$ and against θ for equations (3) and (4). The kinetic and thermodynamic parameters for compounds 3 and 4 are calculated for the first step according to the above two methods and are cited in TABLES 5 and 6. The Thermodynamic parameters, namely entropy (ΔS^*), enthalpy (ΔH^*) and free energy (ΔG^*) of activation were calculated using the following standard relations:

$$\Delta S^* = R [\ln Zh / kT_s] \quad (5)$$

$$\Delta H^* = \Delta E_a - RT_s \quad (6)$$

$$\Delta G^* = \Delta H^* - T_s \Delta S^* \quad (7)$$

where h , Planck's constant, k , Boltzmann constant, R , gas constant and T_s , temperature at the DTG peak.

Negative ΔS^* values for the first stage of decomposition of the complexes suggest that the activated complex is more ordered than the reactants and that the reactions are slower than normal^[29-31]. The more ordered nature may be due to the polarization of bonds in the activated state, which might happen through charge transfer electronic transition^[32]. The different values of ΔH^* and ΔG^* of the complexes refer to the effect of the type of the metal ion on the thermal stability of the complexes^[33]. The lower activation energy of compound 3 compared to that of compound 4 indicates the auto-catalytic effect of copper on the thermal decomposition of the former.

X-ray powder diffraction of the coordination polymers

The X-ray powder diffraction patterns were recorded for the coordination polymers 1, 3, 4 and 5. The diffraction patterns indicate that the compounds

Full Paper

TABLE 5 : Kinetic parameters for the thermal decomposition of the coordination polymers 3 and 4 in dynamic air

Compound	Step	Coats-Redfern equation				Horowitz-Metzger equation			
		r	n	E	Z	r	n	E	Z
3	1 st	0.9926	0.00	33.5	6.74 x 10 ⁻²	0.9929	0.00	31.9	6.48 x 10 ⁻²
		0.9930	0.33	34.7	6.99x 10 ⁻²	0.9935	0.33	33.1	8.86x 10 ⁻²
		0.9931	0.50	35.3	7.11x 10 ⁻²	0.9937	0.50	33.6	10.57x 10 ⁻²
		0.9935	0.66	36.1	7.27x 10 ⁻²	0.9941	0.66	34.2	12.36x 10 ⁻²
		0.9940	1.00	37.3	7.51x 10 ⁻²	0.9946	1.00	35.4	1.68 x 10 ³
		0.9950	2.00	41.4	8.34 x 10 ⁻²	0.9957	2.00	39.2	5.14 x 10 ³
4	1 st	0.9961	0.00	111.2	2.24 x 10 ³	0.9967	0.00	126.6	3.38 x 10 ⁶
		0.9972	0.33	125.5	2.54x 10 ³	0.9977	0.33	141.5	8.67x 10 ³
		0.9977	0.50	133.6	2.71x 10 ³	0.9982	0.50	149.2	1.82x 10 ⁴
		0.9984	0.66	141.2	2.87x 10 ³	0.9985	0.66	157.4	4.02x 10 ⁴
		0.9990	1.00	158.8	3.23x 10 ³	0.9991	1.00	175.3	2.29x 10 ⁵
		1.0000	2.00	216.8	4.36 x 10 ³	0.9992	2.00	223.9	3.86 x 10 ⁷

ΔE_a in kJ mol⁻¹

TABLE 6 : Activation parameters ΔH^* , ΔS^* and ΔG^* of compounds 3 and 4 in dynamic air

Compound	Step	ΔS^*	ΔH^*	ΔG^*
{[Cu(DPP)Cl ₂ (H ₂ O) ₂].4H ₂ O} _n 3	1 st	-197.72	34.30	168.69
{[Cd(DPP)Cl ₂ (H ₂ O) ₂].H ₂ O} _n 4	1 st	-181.57	211.48	116.31

ΔH^* and ΔG^* in kJmol⁻¹ & ΔS^* in Jmol⁻¹K⁻¹

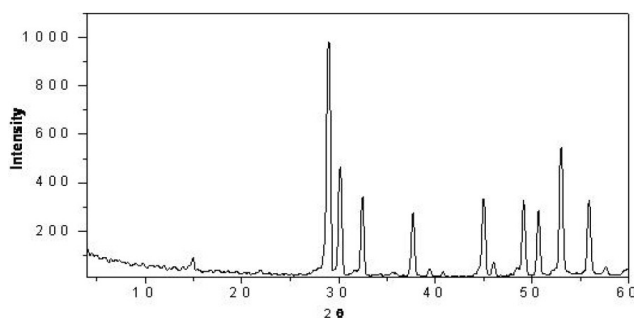


Figure 6 : An XRD pattern of PbO prepared after thermolysis of compound 5

are crystalline. The crystal lattice parameters were computed with the aid of the computer program TREOR. The crystal data for the compounds belong to the crystal system triclinic whereas the residues of compound 3

and 5 belong to the crystal system monoclinic and orthorhombic respectively. The significant broadening of the peaks indicates that the particles are of nanometer dimensions (XRD of compound 5 is depicted in Figure 6). Scherrer's equation (8) was applied to estimate the particle size of the coordination polymers:

$$D = K\lambda / \beta \cos\theta \quad (8)$$

where K is the shape factor, λ is the X-ray wavelength typically 1.54 Å, β is the line broadening at half the maximum intensity in radians and θ is Bragg angle and D is the mean size of the ordered (crystalline) domains, which may be smaller or equal to the grain size. The crystal data together with particle size are recorded in TABLE 7. The average size of the particles lies in the range 19-27 nm for the compounds and in the range 22-36 nm for the residues which are in close agreement with that calculated from SEM and TEM photographs.

Scanning electron micrographs (SEM)

The scanning electron micrographs of compounds 3, 4 and 5 as representatives are given in Figures 7-11.

TABLE 7 : X-ray powder diffraction crystal data of the compounds and their particle size

Compound	a (Å)	b (Å)	c (Å)	α	β	γ	Volume of Unit Cell(Å ³)	Crystal System	Particle Size(nm)
1	4.740	16.651	18.410	39.260	78.469	106.191	644.15	Triclinic	27
3	6.903	9.033	15.241	65.961	113.750	69.890	631.10	Triclinic	19
4	4.289	9.836	22.879	67.058	76.913	95.385	847.97	Triclinic	24
5	8.927	9.042	10.431	85.363	75.002	129.454	593.09	Triclinic	23
[CuO]	4.662	3.416	5.118	90.00	99.49	90.00	-	Monoclinic	22
[PbO]	5.612	5.608	4.992	90.00	90.00	90.00	-	Orthorhombic	36

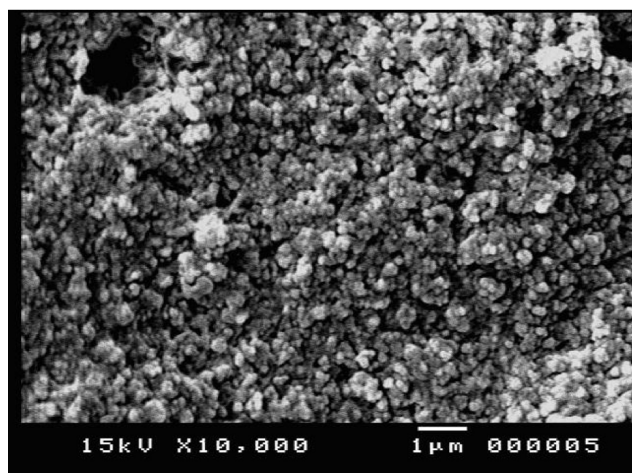


Figure 7 : SEM of $\{[\text{Cu}(\text{DPP})\text{Cl}_2(\text{H}_2\text{O})_2] \cdot 4\text{H}_2\text{O}\}_n$

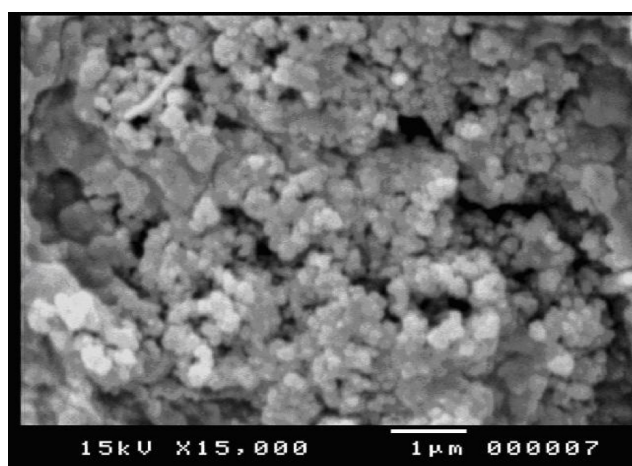


Figure 8 : SEM of $\{[\text{Cd}(\text{DPP})\text{Cl}_2(\text{H}_2\text{O})_2] \cdot \text{H}_2\text{O}\}_n$

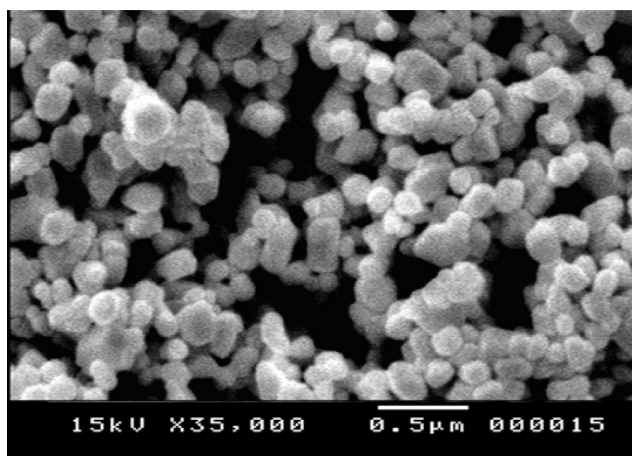


Figure 9 : SEM photographs of $[\text{Pb}(\text{DPP})(\text{NO}_3)_2(\text{H}_2\text{O})_2]_n$

The figures show the different morphologies of the coordination polymers. The packing of the structures on a molecular level might have affected the morphology of the nano-structure of the compounds. It is clear from the SEM figures of the coordination polymers that the prepared thin films produce compounds of regular

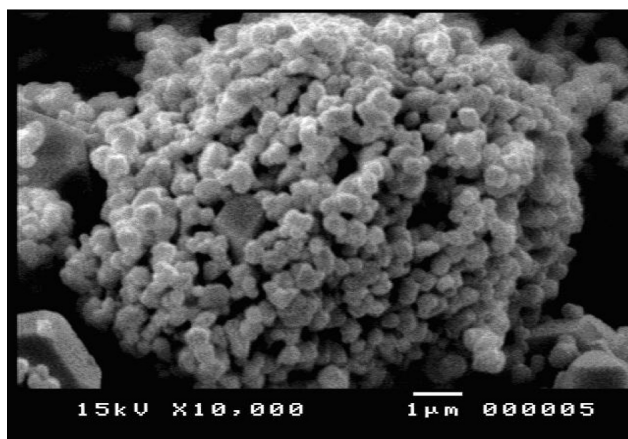


Figure 10 : SEM photographs of PbO nanospheres (produced by calcination of compound 5)

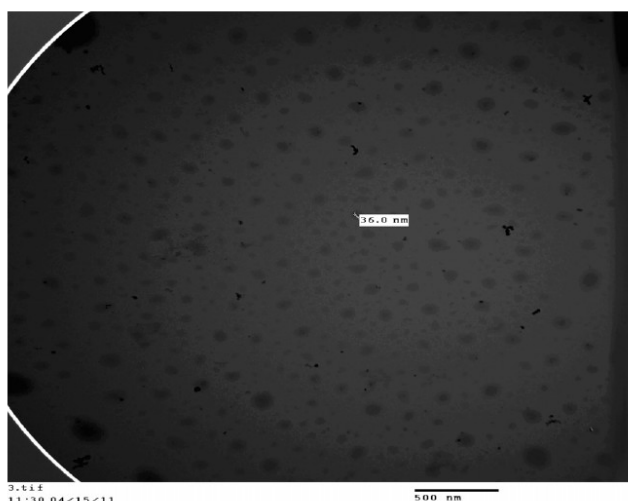


Figure 11 : TEM photographs of PbO nanospheres (produced by calcination of compound 5)

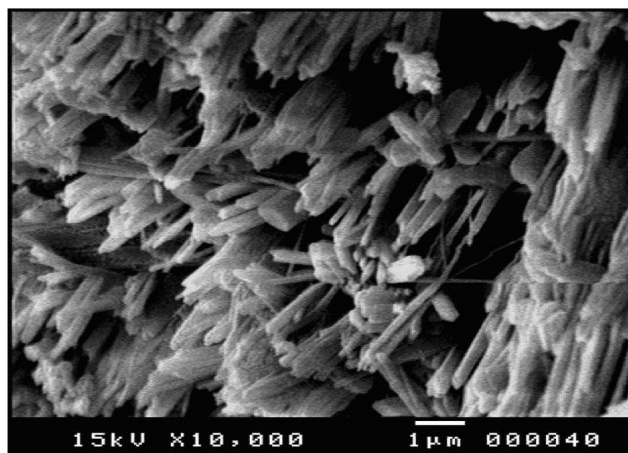


Figure 12 : SEM photographs of CuO nanorods (produced by calcination of compound 3)

shaped nanoparticles. These compounds function then as precursors for nanooxides (Figures 10, 11 and 12). The SEM photograph of CuO shows the rod shaped

TABLE 8 : Microbiological screening of the compounds

Compound	<i>B. Cereus</i> (G+ve)	<i>S. aureus</i> (G+ve)	<i>S. Marcescens</i> (G-ve)	<i>E.coli</i> (G-ve)	<i>P. aeruginosa</i> (G-ve)	<i>A. flavus</i>	<i>C. albicans</i>	<i>F. oxysporm</i>	<i>G. candidum</i>	<i>S. brevicaulis</i>
2	16	13	12	15	14	0	14	0	22	0
4	17	11	10	11	11	15	12	0	20	18
5	0	0	0	0	0	0	0	0	12	0

nanoparticles. The SEM and TEM photographs of PbO indicate the regular shape of the nanoparticles.

Microbiological screening

The antimicrobial activity of compounds 2, 4 and 5 was tested against 5 bacterial and 5 fungal strain (TABLE 8). As shown in the table compounds 2 and 4 exhibited a broad spectrum of the antibacterial action with the highest activity observed against *Bacillus cereus* (Gram +ve) and the lowest towards *Serratia marcescens*

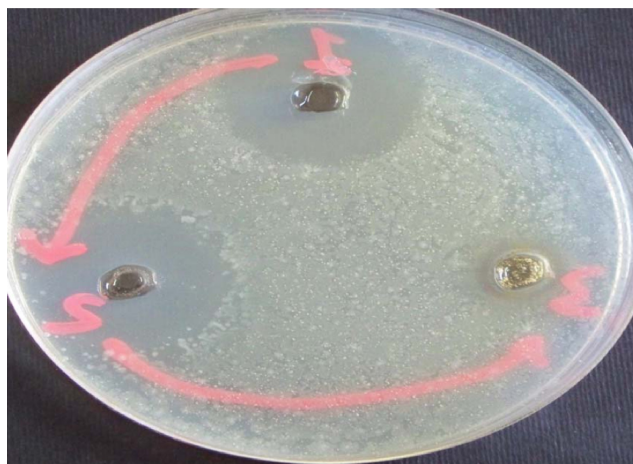


Figure 13 : Microbiological screening of compounds 2 and 4 against *Bacillus cereus*

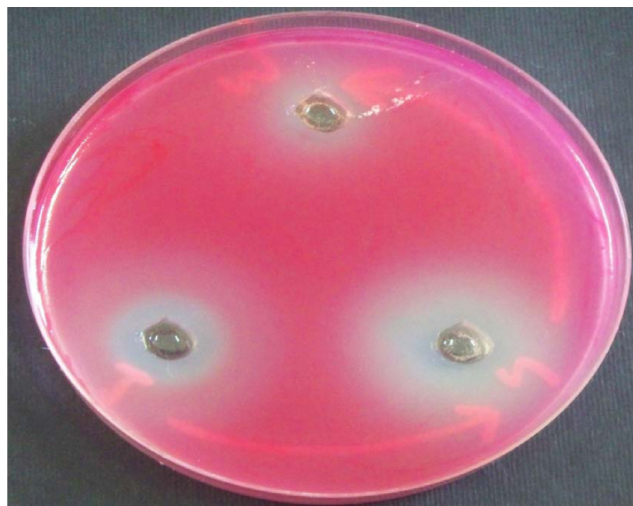


Figure 14 : Microbiological screening of compounds 2 and 4 against *Serratia marcescens*



Figure 15 : Microbiological screening of compounds 2, 4 and 5 against *Geotrichum Candidum*

(Gram –ve). On the other hand, all bacterial strains were resistant to compound 5. Concerning the antifungal activity, these compounds were effective against *Geotrichum Candidum* (a yeast like human pathogen fungus) with the highest inhibitory activity exerted by compound 2 and the lowest by compound 5. *Candida albicans* (also a yeast like human pathogen fungus) was inhibited by compounds 2 and 4, but it was resistant to compound 5. Compound 4 inhibited also the growth of *Scopulariopsis brevicaulis* and *Aspergillus flavus*. (Figures 13-15).

ACKNOWLEDGEMENT

One of the authors (A. A. M. ALY) is very grateful to Alexander Von Humboldt Foundation for donating the magnetic susceptibility balance (MSB-Auto).

REFERENCES

- [1] M.Fujita, Y.J.Kwon, S.Washizu, K.Ogura; J.Am.Chem.Soc., **116**, 1151-1152 (1994).
- [2] O.M.Yaghi, H.Li, C.Davis, D.Richardson, T.L.Groy; Acc.Chem.Res., **31**, 474-484 (1998).

- [3] J.S.Seo, D.Whang, H.Lee, S.I.Jun, J.Oh, Y.J.Jeon, K.Kim; *Nature*, **404**, 982-986 (2000).
- [4] S.Q.Ma, X.S.Wang, D.Q.Yuan, H.C.Zhou; *Angew.Chem.Int.Ed.*, **47**, 4130-4133 (2008).
- [5] H.Sadeghzadeh, A.Morsali, V.Yilmaz, O.Buyukgungor; *Ultra.Sonochem.*, **17**, 592-597 (2010).
- [6] A.Aslani, A.Morsali, M.Zeller; *Solid State Sciences.*, **10**, 1591-1597 (2008).
- [7] P.K.Arcot, J.Luo; *Surf.Coat.Technol.*, **202**, 2690-2697 (2008).
- [8] P.K.Arcot, J.Luo; *Mater.Lett.*, **62**, 117-120 (2008).
- [9] G.Bhagavannarayana, S.K.Kushwaha, S.Parthiban, G.Ajitha, S.Meenakshisundaram; *J.Cryst.Growth*, **310**, 2575-2583 (2008).
- [10] M.Rubner; *Nature*, **423**, 925-926 (2003).
- [11] L.F.Marques, M.V.Marinho, N.L.Speziali, L.C.Visentin, F.C.Machado; *Inorg.Chem.Acta.*, **365**, 454-457 (2011).
- [12] M.T.Bujaci, X.Wang, S.Li, C.Zheng; *Inorg.Chim.Acta.*, **333**, 152-154 (2002).
- [13] M.G.Amiri, Z.R.Ranjbar, A.Morsali, V.T.Yilmaz, O.Buyukgungor; *Solid State Sci.*, **8**, 1115-1120 (2006).
- [14] (a) M.J.Plater, M.R.St, J.Foreman, T.Gelbrich, S.J.Coles, M.B.Hursthouse; *J.Chem.Soc.Dalton Trans*, 3065-3073 (2000); (b) M.J.Plater, M.R.St, J.Foreman, T.Gelbrich, M.B.Hursthouse; *Inorg.Chim.Acta*, **318**, 171-174 (2001).
- [15] Xi.L.Wang, Y.Lu, H.Fu, J.X.Meng, E.B.Wang; *Inorganica Chimica Acta*, **370**, 203-206 (2011).
- [16] M.Atsuchi, K.Inoue, S.Nakashima; *Inorganica Chimica Acta*, **370**, 82-88 (2011).
- [17] H.B.Xiong, D.Sun, G.G.Luo, R.B.Huang, J.C.Dai; *J.Mole.Stru.*, **990**, 164-168 (2011).
- [18] W.J.Geary; *Coord.Chem.Rev.*, **7**, 81-122 (1971).
- [19] J.Q.Liu, W.P.Wu, Y.Y.Wang, W.H.Huang, W.H.Zhang, Q.Z.Shi, J.S.Miller; *Inorg.Chim.Acta*, **362**, 1291-1295 (2009).
- [20] L.Hashemi, A.Morsali, P.Retailleau; *Inorganica Chimica Acta*, **367**, 207-211 (2011).
- [21] T.Rakha; *Synth.React.Inorg.Met.Org.Chem.*, **30**, 205-224 (2000).
- [22] A.Bravo, J.Anacona; *Transition.Met.Chem.*, **26**, 20-23 (2001).
- [23] R.L.Dutta, A.Syamal; *Elements of Magnetochemistry*, Second Edition, Affiliated East-west Press, New Delhi, 34 (1993).
- [24] S.Song, T.Xiao, C.Redshawb, X.Hao, F.Wang, W.Sun; *J.Organo.Chem.*, **696**, 2594-2599 (2011).
- [25] J.R.Anacona, C.Toledo; *Transition Met.Chem.*, **26**, 228-231 (2001).
- [26] A.Sabastiyani, D.Venkappayya; *J.Ind.Chem.Soc.*, **67**, 584-589 (1990).
- [27] A.Coats, J.Redfern; *Nature.*, **20**, 68-69 (1964).
- [28] H.Horowitz, G.Metzger; *Anal.Chem.*, **35**, 1464-1468 (1963).
- [29] G.G.Mohamed, W.M.Hosny, M.A.Abd El-Rahim; *Synth.React.Inorg.Met.Org.Chem.*, **32**, 1501-1519 (2000).
- [30] M.A.A.Beg, M.A.Qaiser; *Thermochim. Acta.*, **210**, 123-132 (1998).
- [31] J.Hill, R.J.Magee; *Reviews Inorg.Chem.*, **3**, 141-197 (1981).
- [32] K.K.M.Yusuff, A.R.Karthikeyan; *Thermochim. Acta.*, **207**, 193-199 (1992).
- [33] M.E.Emam, M.Kanawy, M.H.Hafe; *J.Therm.Anal. Cal.*, **63**, 75-83 (2001).